Multimetallic Lithium Complexes Derived from the Acids $Ph_2C(X)CO_2H$ (X = OH, NH_2): Synthesis, Structure and Ring Opening Polymerization of Lactides and Lactones

Yahya F. Al-Khafaji,[a] Dr. Timothy J. Prior,[a] Dr. Lynne Horsburgh,[b] Dr. Mark R. J. Elsegood[b] and Prof. Carl Redshaw[a*]

[a] *Department of Chemistry, The University of Hull, Cottingham Rd, Hull, HU6 7RX, U.K.*

[b] *Chemistry Department, Loughborough University, Loughborough, Leicestershire, LE11 3TU, U.K.*

E-mail: C.Redshaw@hull.ac.uk

Abstract Reaction of LiOR (R = *t*-Bu, Ph) with the acids 2,2′-$Ph_2C(X)(CO_2H)$, X = OH (benzH), NH_2 (pdgH) was investigated. For benzH, one equivalent LiO*t*-Bu in THF afforded $[Li(benz)(THF)]_2 \cdot 2THF$ (**1**·2THF), which adopts a 1D chain structure. If acetonitrile is used (mild conditions), another solvate of **1** is isolated**;** LiOPh also led to **1**. Robust work-up afforded $[Li_7(benz)_7(MeCN)]$ (**2**·2MeCN·THF). Use of LiO*t*-Bu (2 equivalents) led to $\{Li_8(O\textit{t}\text{-}Bu)_2[(benz)](OCPh_2CO_2CPh_2CO_2\textit{t}\text{-}Bu)_2(THF)_4\}$ (**3**), the core of which comprises two open cubes linked by benz ligands. For dpgH, two equivalents of LiO*t*-Bu in THF afforded $[Li_6(O\textit{t}\text{-}Bu)_2(dpg)_2(THF)_2]$ (**4**), which contains an Li_2O_2 6-step ladder. Similar reaction of LiOPh afforded $[Li_8(PhO)_4(dpg)_4(MeCN)_4]$ (**5**). Complexes **1 - 5** were screened for their potential as catalysts for ring opening polymerization (ROP) of ε-caprolactone (ε-CL), *rac*-lactide (*rac*-LA) and δ-valerolactone (δ-VL). For ROP of ε-CL, conversions > 70% were achievable at 110 ^oC with good control. For *rac*-LA and δ-VL, temperatures of at least 110 ^oC over 12h were necessary for activity (conversions > 60%). Systems employing **2** were inactive.

Introduction

Over the last decade, there has been a great deal of interest in the ring opening polymerization (ROP) of cyclic esters as a route to accessing biodegradable polymers. Polymers which have attracted particular interest include polycaprolactone (PCL) and polylactide (PLA), and to a lesser extent polyvalerolactone (PVL). Applications of such polymers are widespread and include use in the medical arena, for example as biodegradable implants, and use in the packaging industry.[1] Coordination chemistry plays a central role in this field by allowing for the development of new, efficient, metal-based initiators by manipulation of the coordination environment about the metal centre.[2] In other words, the choice of both the metal centre and the ligand set is crucial in terms of being able to control the features associated with the ROP process such as catalytic activity (% conversion) and the resultant polymer properties. The use of chelating and/or bulky ligands with a variety of metals has proved particularly successful.[2] We have been investigating the use of ligands derived from acids bearing the motif $Ph_2(X)CO_2H$, where X = OH, NH_2, and have previously reported some intriguing molecular structures.[3] The ability of this motif to promote highly crystalline samples was first recognised by Braun.[4] More recently, we have investigated organoaluminium complexes bearing ligands derived from such acids, and have exploited them in terms of their capability for the ROP of cyclic esters.[5] A search of the CSD for compounds incorporating the $Ph_2C(X)$ motif revealed only a limited number of compounds (<40), the majority of which contained no metal.[6] We are also interested in the use of alkali metal species for ROP, given that their use in a number of systems has resulted in promising results with little in the way of side reactions.[7] With this in mind, and given the aforementioned limited coordination chemistry of acids containing the $Ph_2C(X)$ motif, we report here our investigations on the use of lithium complexes bearing ligands derived from $Ph_2(X)CO_2H$, which as well as resulting in some unusual structural motifs incorporating lithium-oxygen rings and ladders (see scheme 1), has afforded ROP systems exhibiting reasonable activities and low polydispersities (PDIs). We note that a number of lithium-containing cages, rings and ladders, supported primarily by phenolate-type ligation, have previously been employed for the ROP of cyclic esters.[7, 8]

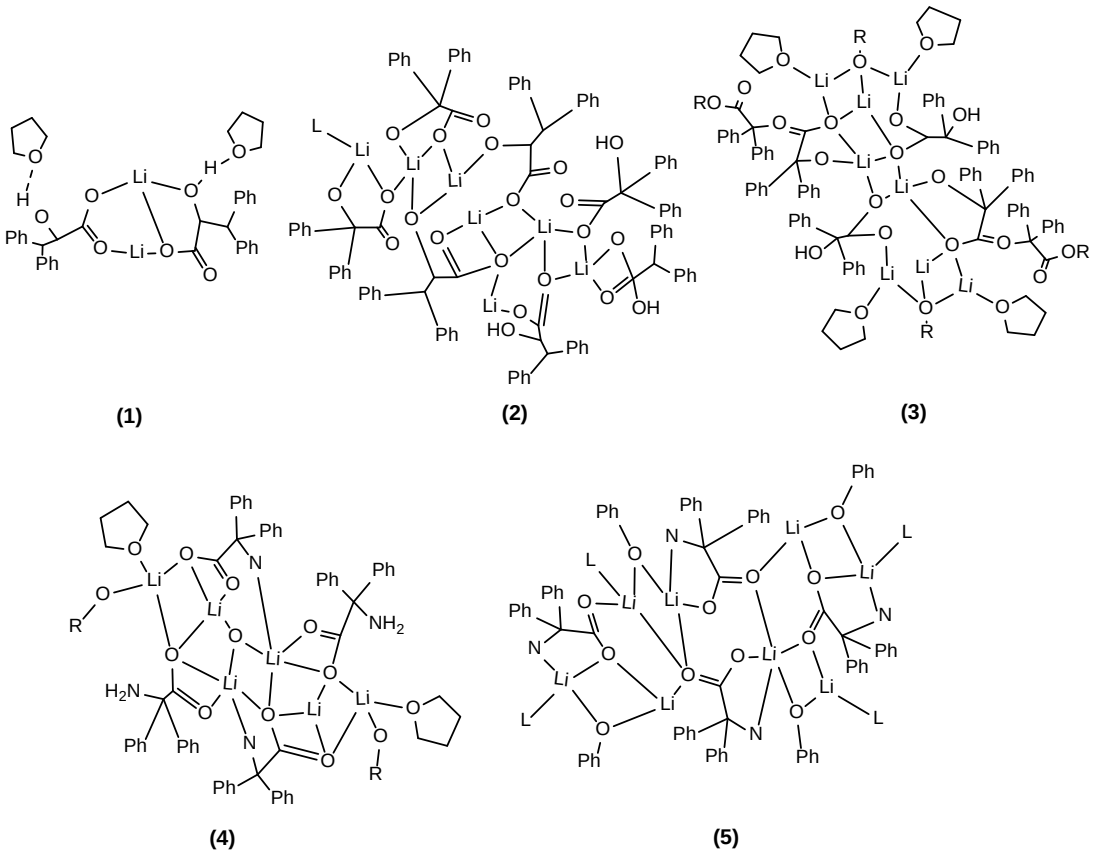

Ph= phenyl, R= ^{t}Bu, L=MeCN

Scheme 1

Results and Discussion

Use of benzylic acid

Our initial studies have focused on the use of benzilic acid, benzH, given it is available in bulk quantities at relatively low cost.[9] Using a 1:1 mole ratio of benzH and lithium *tert*-butoxide in THF afforded, following work-up, colourless prisms $[Li(benz)(THF)]_2 \cdot 2THF$ (**1**·2THF) in moderate yield. Single crystals suitable for X-ray diffraction were obtained upon prolonged standing (2 – 3 days) at ambient temperature. The molecular structure is shown in figure 1 (also see figures S1 – S4, SI), with selected bond lengths and angles given in the caption. The structure is best described as mono-deprotonated benzilic acid which via Li^+ coordination forms 1D chains. The chains comprise a number of fused 5- and 6-membered rings along the chain/ladder, rather than the more commonly observed Li_2O_2 diamond-like motifs. Both Li1 and Li2 are

four coordinate, with distorted tetrahedral geometry and are bound by an 'acid' oxygen from each of three benz ligands plus the hydroxyl from one of them. The Li – O bond lengths [1.905 (5) - 1.965 (6) Å] are comparable with other bimetallic lithium systems in the literature,[10] with those to the μ^3-O atoms O(2) and O(4) being the longest. The carboxylate at C(1) binds in *syn* fashion. The O–H hydrogens of both benz ligands are involved in H-bonding to THF which resides in clefts along the chain (see Figure S1, SI).

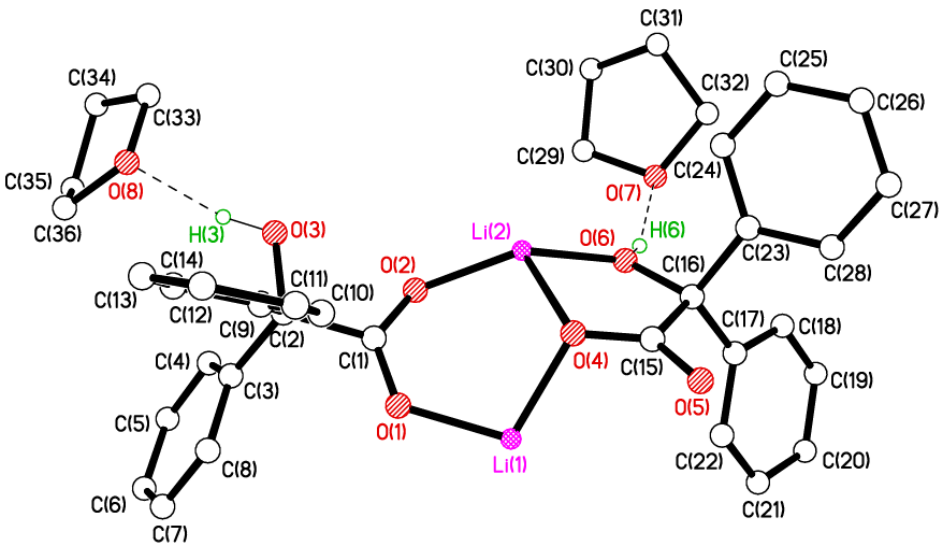

Figure 1. The asymmetric unit in the 1D chain structure of **1**·2THF. Selected bond lengths (Å) and angles (°): Li(1)–O(1) 1.905(5), Li(1)–O(2′) 1.935(5), Li(1)–O(4) 1.926(6), Li(2)–O(2) 1.965(6), Li(2)–O(4) 1.964(5), Li(2)–O(5′) 1.953(6), Li(2)–O(6) 1.949(6); Li(1)–O(2)–Li(2′) 107.8(2), Li(1)–O(4)–Li(2) 111.6(2), O(6)–Li(2) – O(4) 80.4(2).

In the packing of the **1**, the 1D chains are aligned parallel to the crystallographic *a* direction. Neighbouring chains connect via van der Waals forces only (see SI, figures S2 and S3).

Conducting the same reaction, but utilising acetonitrile (MeCN) during work-up under mild conditions, (stirring at room temperature for 10 mins) afforded crystals with two distinct morphologies, namely small needles together with much larger blocks in approximately 70:30 ratio. Both morphologies were subjected

to single crystal X-ray diffraction and gave different unit cells, one of which matched **1**. Both structures are 1D polymers, and in each phase, each lithium is surrounded by four oxygen atoms in a flattened tetrahedron. The key difference is in the location of the THF and associated composition and geometry of the Li-benz chain. For **1**, the THF is not bound to Li^+ but is localised by a hydrogen bond from the alcohol of benzilic acid. The chain is composed of five- and six-membered rings.

The structure of the second polymorph **1′**, which crystallises in the chiral space group $P2_12_12_1$ with a single lithium ion, one benzilic acid and one molecule of THF in the asymmetric unit, could be described as a chain made up from discrete Li(benz)(THF) moieties in which the benzilic acid is bound to Li(1) through a single oxygen of the carboxylate and the alcohol in a 5-membered chelate ring, in other words the benzilic acid is bidentate to the lithium through the O(1) of the carboxylate and the alcohol O(3). The same oxygen atom of the carboxylate also coordinates to a second Li(1) ion generated by symmetry (the so-called monatomic bridging coordination mode). Critically, in this polymorph, the THF is bound to the Li^+ (see figure 2).

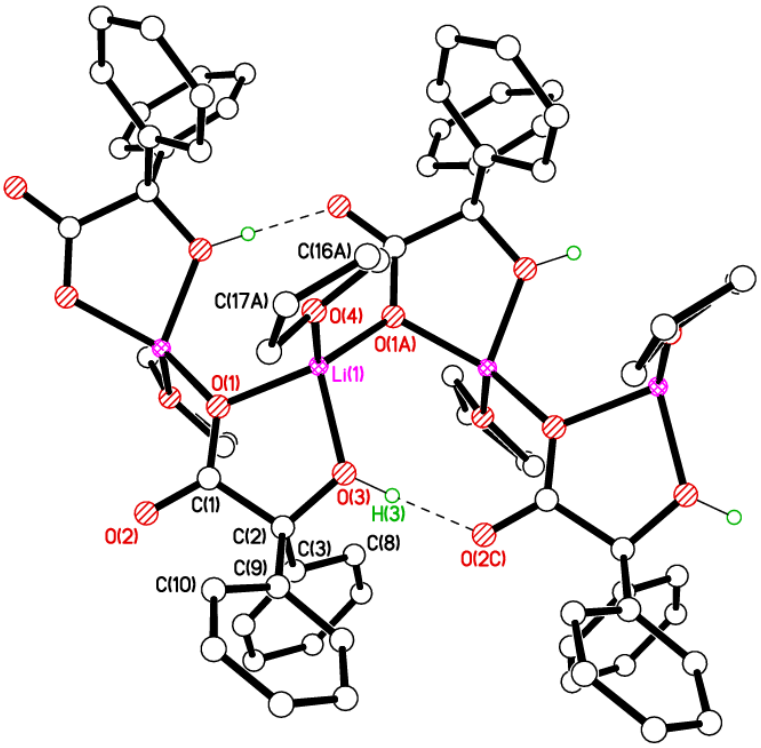

Figure 2. Coordination about Li(1) in **1′** and H-bonds supporting the chain structure. Selected bond lengths (Å) and angles (°): Li(1)–O(1) 1.926(4), Li(1)–O(1A) 1.900(3), Li(1)–O(3) 1.917(3), Li(1)–O(4) 1.962(4); O(1)–Li(1)–O(1A) 134.88(19), O(1)–Li(1)–O(3) 82.99(13), O(3)–Li(1)–O(4) 109.95(17).

The coordination of the lithium is completed by another O(1) atom generated by symmetry to give a tetrahedral arrangement of oxygen atoms. This generates a zig-zag chain composed of Li(1) and O(1) atoms that runs parallel to the crystallographic *a* direction (figure 3). O(2) takes no part in binding to Li(1).

There is a hydrogen bond between H(3) and O(2) of a neighbouring benzylic acid. This hydrogen bond is approximately along the *a* direction, strengthening the chain.

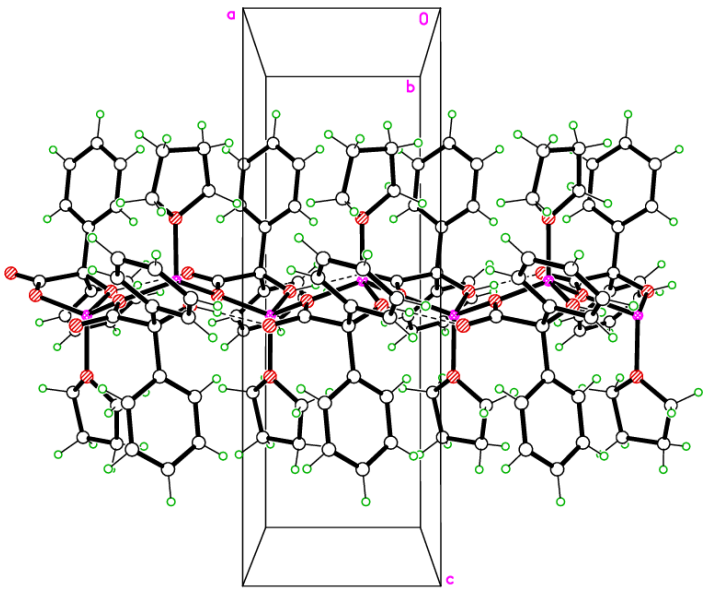

Figure 3. Chains in **1′** which are all aligned along *a*, are arranged in a square grid in the *bc* plane. Between the chains there are no classic hydrogen bonds but there is evidence for C−H···π interactions between the benz ligands and THF. This view is orthogonal to that in figure 2 above.

If, during work-up when employing LiO*t*Bu, the complex is recrystallized from acetonitrile after 10 mins of refluxing, then the complex $[Li_7(benz)_7(MeCN)]$ (**2**·2MeCN·THF) is formed. In this case, the asymmetric unit contains three molecules of acetonitrile, one of which coordinates to Li. The crystal structure of **2** (figure 4) was determined using synchrotron radiation (for alternative view see figure S4, SI); the crystal was weakly scattering and has a large asymmetric unit but displays a beautiful structure. The structure crystallises in the centrosymmetric space group $P2_1/n$ with 140 crystallographically-unique non-hydrogen atoms in the asymmetric unit.

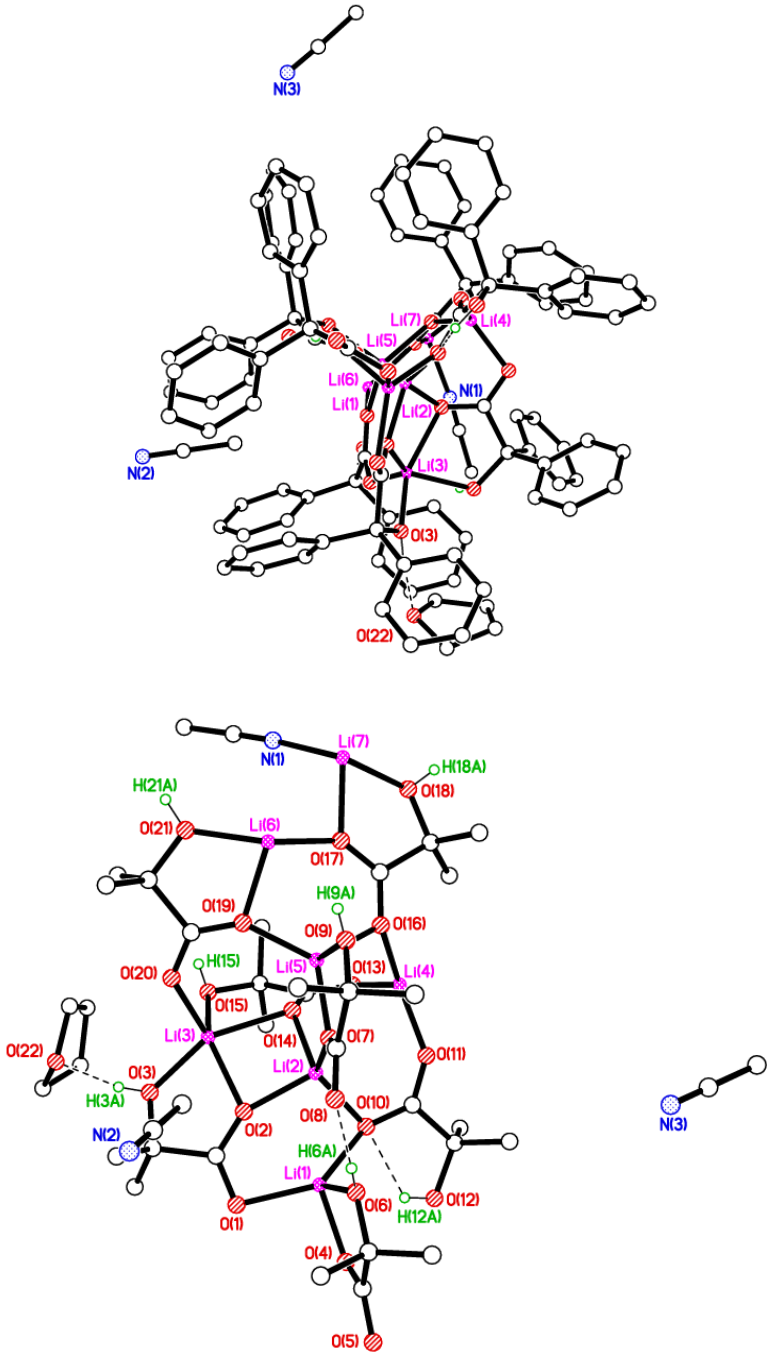

Figure 4. Two approximately orthogonal views of the asymmetric unit of chain polymer **2**. Selected bond lengths (Å) and angles (°): Li(1)–O(1) 2.052(3), Li(2)–O(2) 1.933(3), Li(3)–O(3) 1.994(4), Li(4)–O(13) 1.830(5), Li(5)–O(9) 2.032(4), Li(6)–O(7) 1.971(3), Li(7–O(18 1.982(3); Li(1)–O(10)–Li(2) 85.1(1), Li(2)–O(2)–Li(3) 88.4(2), Li(2)–O(14)–Li(3) 86.3(2), Li(2)–O(7)–Li(5) 95.9(1), Li(4)–O(16)–Li(5) 101.4(2), Li(5)–O(19)–Li(6) 99.2(1), Li(6)–O(17)–Li(7) 97.8(1).

The benzilates bind to lithium through the carboxylate and through the alcohol. The carboxylate is observed as bridging bidentate [*e.g.* O(1)–C(1)–O(2)] and also mono-dentate coordination where a single oxygen of the carboxylate binds to two lithium ions [*e.g.* O(7)]. In this case, the free C=O carbonyl is stabilised by a hydrogen bond from the alcohol. [*e.g.* O(6)−H(6)···O(8)]. The three centres Li(1), Li(2), Li(3) adopt a distorted square-based pyramidal geometry surrounded by 5 oxygen atoms, whilst Li(5) and Li(6) adopt a distorted trigonal bipyramidal geometry. Li(7) adopts a distorted square planar geometry, with the apical position occupied by $NCCH_3$.

There are four oxygen atoms around Li(4) in a trigonal pyramidal arrangement, with apparently vacant space at the base of this pyramid. This ion is not really naked as it lies directly below one of the C–H bonds of a benzilic acid [Li(4)···C(84) = 2.715(5) Å; Li(4)···H(84) = 2.81 Å] at a distance of 2.689(5) Å from the mean plane of the phenyl ring.

The arrangement of lithium ions coordinated by benzilates leads to tapes that run in the [101] direction (figure 5). Each tape is essentially a linear arrangement of five unique Li ions bridged by benzilic acid that is augmented by two further lithium ions and further benzilic acid. The tapes are packed in layers parallel to the *ac* plane; layers are packed ABAB parallel to *b*.

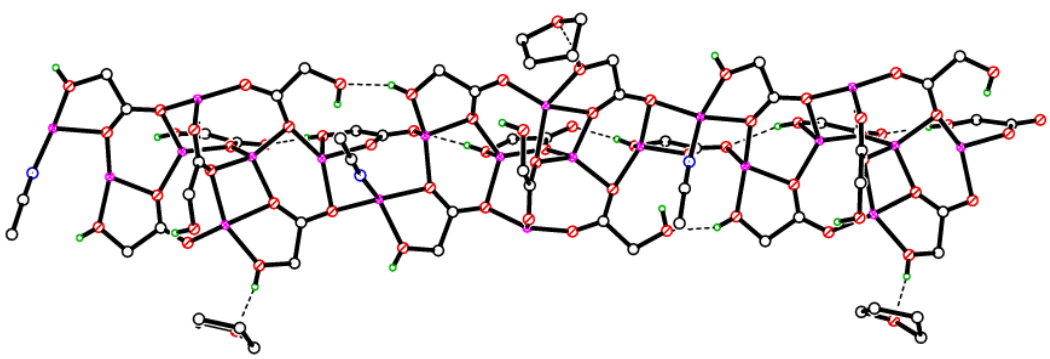

Figure 5. Portion of a single tape of **2** that runs parallel to the [101] direction.

Conducting the reaction under similar conditions, but using a 1:2 mole ratio of benzH and lithium *tert*-butoxide afforded a somewhat different complex, namely $[Li_8(benz)_2(O\textit{t}\text{-}Bu)_2(OC(Ph)_2CO_2C(Ph)_2CO_2\textit{t}\text{-}Bu)_2(THF)_4]$ (**3**). The molecular structure is shown in figure 6 (for alternative view see figure S5, SI), with selected bond lengths and angles given in the caption.

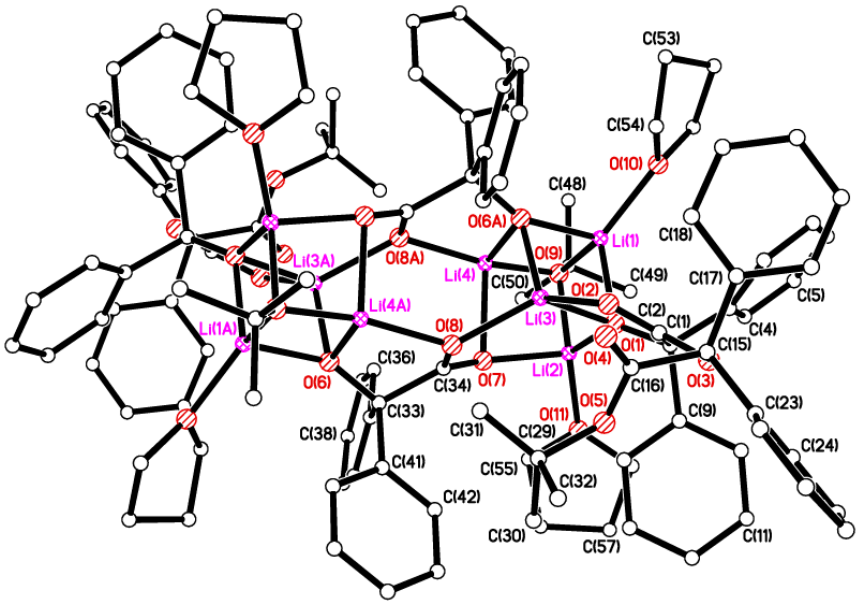

Figure 6. Molecular structure of **3**. Selected bond lengths (Å) and angles (°): Li(1)–O(1) 2.000(9), Li(1)–O(9) 1.948(9), Li(1)–O(10) 1.991(9), Li(2)–O(1) 1.917(9), Li(2)–O(7) 1.961(9), Li(3)–O(1) 1.959(9), Li(3)–O(2) 2.040(9), Li(3)–O(8) 2.052(9), Li(4)–O(9) 1.892(8); O(9)–Li(1)–O(10) 133.0(5), Li(1)–O(1)–Li(3) 82.0(3), Li(2)–O(1)–Li(3) 98.9(4), Li(1)–O(9)–Li(4 83.6(4), Li(2)–O(9)–Li(4) 86.9(3).

Half of the formula is the asymmetric unit because the molecule sits on a centre of symmetry. Two open cubes are linked by a pair of deprotonated benzilic acids. Each half of the molecule contains four different types of lithium centre. Li(1) and O(1) are bound by a bridging chelate ligand which formally results from the coupling of two benz and a *tert*-butoxide ligand. A search of the CSD revealed no examples of this type of coupled motif. [6] Within the central core, the Li – O bonds are in the range 1.892(8) – 2.142(8) Å, with

the longest associated with the μ_3 atoms O(7) and O(8). In **3**, there are no significant intermolecular interactions (or H-bonding).

Use of 2,2′-diphenylglycine

Having established suitable synthetic condition for the synthesis and isolation of lithium complexes derived from $Ph_2C(OH)CO_2H$, we extended our studies to the somewhat more expensive 2,2′-diphenylglycine, $Ph_2C(NH_2)CO_2H$ (dpgH). [9] Using 1:2 mole ratio from dpgH and lithium *tert*-butoxide led to the isolation of the complex $[Li_6(O\textit{t}\text{-Bu})_2(dpg)_4(THF)_2]$ (**4**). In the infrared spectrum, ν_{NH} stretching modes are detected at approximately 3358, 3296 and 3159 cm^{-1}. The molecular structure is shown in figure 7 (and figure S6, SI). Half of this formula comprises the asymmetric unit, and the molecule lies on a centre of symmetry. The core of the molecule comprises an Li_2O_2 ladder which has 6 steps supported by four dpg-derived ligands and two *tert*-butoxides. Such Li_2O_2 ladders are common in lithium chemistry and can varying in the number of steps present. Indeed, a search of the CSD revealed 26 hits for Li_2O_2 containing ladders; there were another 205 hits for Li–O containing cages (including cubes).[6] In **4**, there is intramolecular H-bonding: N(1)–H(1A)···O(1) (Table S1, SI).

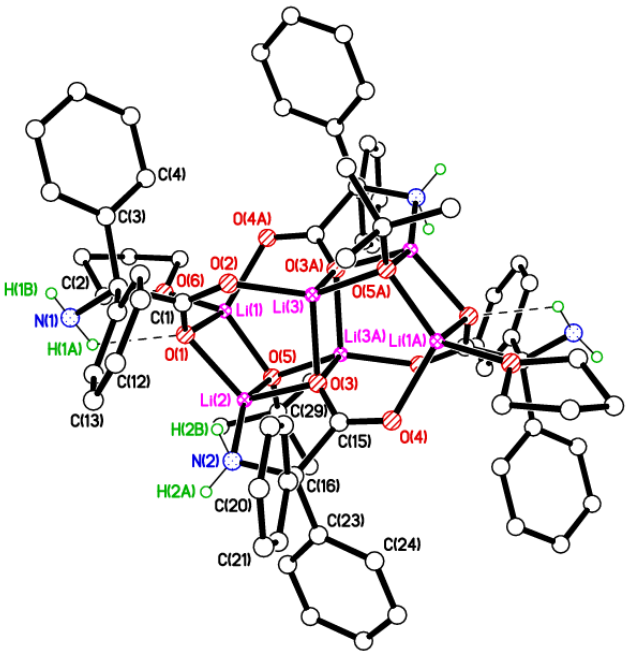

Figure 7. The molecular structure of **4**. Selected bond lengths (Å) and angles (°): Li(1)–O(5) 1.910 (11), Li(1)–O(6) 1.960(11), Li(1)–O(4) 1.972(10), Li(2)–O(3) 1.952(10), Li(2)–O(5) 1.898(10), Li(2)–N(2) 2.122(11), Li(3)–O(2) 1.879(10), Li(3)–O(3) 2.006(10); O(5)–Li(1)–O(6) 124.4(5), O(5)–Li(2)–O(3) 98.2(4), O(2)–Li(3)–O(3) 103.8(4).

Furthermore, molecules of **4** are linked into 1D chains via head-to-tail pairs of intermolecular H-bonds N(2′)–H(2B′)···N(1). The chains run parallel to *a* (figure 8). However, there are no significant interactions between chains.

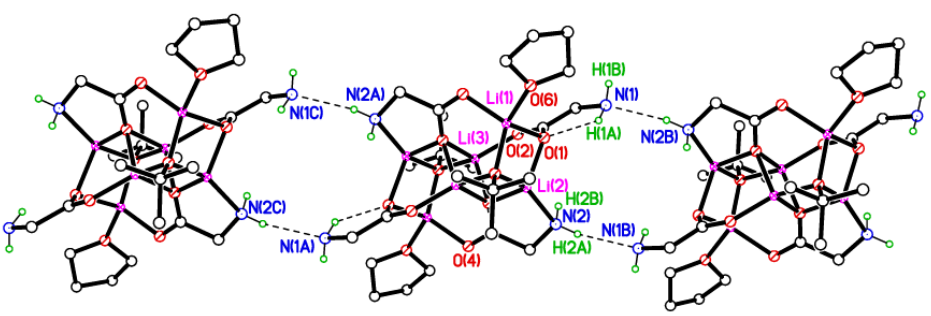

Figure 8. Chains of **4** parallel to *a*.

Using 1:2 mole ratio from dpgH and lithium phenoxide results in a product for which the asymmetric unit contains two symmetry-unique portions each of composition Li_2:dpg:phenoxide:MeCN (**5**). The overall structure is best viewed (figure 9) as an 8×Li cluster with formula $[Li_8(dpg)_4(phenoxide)_4(MeCN)_4]$. Clusters of **5** are essentially an Li_8O_8 core that is formed from four Li_2O_2 square planes arranged alternately by rotation of 90 °degrees to give a Li_8O_8 capsule. This capsule is then further stabilised by the nitrogen ligands (bidentate dpg) around the central portion of the capsule at 90 ° to each other (like sails on a windmill). The capsules are terminated by mono-dentate acetonitrile. For an alternative view of **5**, see figure S7 (SI).

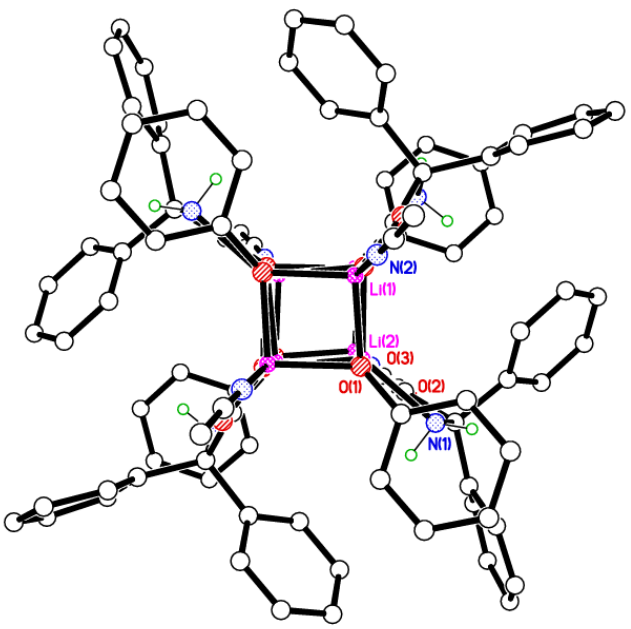

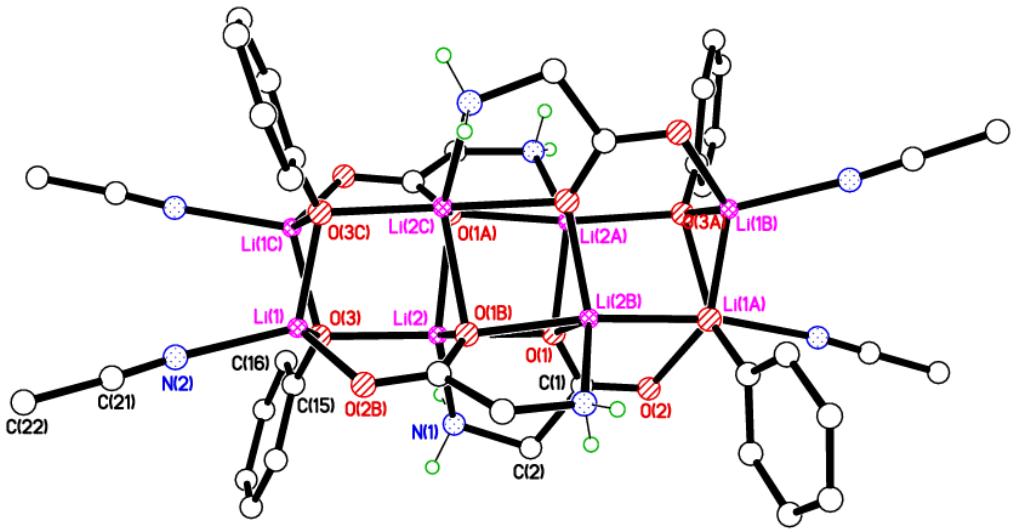

Figure 9. Two orthogonal views of the molecular structure of **5**·4MeCN. Selected bond lengths (Å) and angles (°): Li(1)–O(3) 1.920(15), Li(1)–N(2) 2.103(14), Li(2)–O(1) 2.003(15), Li(2)–O(3) 2.064(12), Li(2)–N(1) 2.151(15); Li(1)–O(3)–Li(2) 100.9(6), O(3)–Li(1)–N(2) 113.0(3), N(1)–Li(2)–O(1) 75.9(5). DPG Ph groups have been omitted for clarity in the lower figure.

In solution, complexes **1** – **5** exhibit only a single peak in their ^{7}Li NMR spectra, which is consistent with the disaggregation observed by O'Hara, Kozak and Kerton.[8d, h, i]

Ring opening polymerization (ROP)

ROP of ε-caprolactone

Complexes **1** – **5** have been screened for their ability to ring open polymerize ε-caprolactone (in the presence of benzyl alcohol (BnOH) in case of **1**). Complex **4** was selected to determine the optimum conditions (table 1), and the results revealed that this catalyst was most effective for the ROP of **ε**-CL at temperatures of 80 to 110 °C. According to the entries (12-17, table 1), there is a near exponential relationship between monomer conversions and M_n values (Fig. S8, SI), possibly due to severe catalyst decomposition, with molecular weight distributions [1.13 – 1.66] that suggest there is some degree of control. There is an approximate linear relationship between conversion ratio and average molecular weight

(M_n), which suggests the system still retains the classical features of a living polymerization process (Fig. S9, ESI). In the ^{1}H and ^{13}C NMR spectra of the PCL (table 1, run 6, figures S10 and S11), no peaks associated with end groups could be identified. This suggests the formation of cyclic PCL; this has been noted previously when using pre-catalysts containing Li/O rings.[6g] The MALDI TOF spectrum of the PCL (figure S12) revealed peaks separated by 114 mass units (the molecular weight of the monomer ε-CL).

The ROP of ε-CL in the absence of solvent was also investigated (table S2). Higher conversions were achieved over short time periods, but at the expense of (i.e. lower) observed M_n values for the respective pre-catalysts; PDIs were in the range 1.21 to 2.01.

From a kinetic study of the ROP of ε-CL using **1** and **3 - 5** (figure 10), it was observed that the polymerization rate exhibited first order dependence on the CL concentration (figure 10, left), and the conversion of monomer achieved was >80 % over 100 min (figure 10, right). Figure 10 indicates that the rate order is **3** > **4** > **5** > **1** (table S3) suggesting that for **3** and **4**, the presence of the O-*t*Bu and/or THF ligation at lithium may well be beneficial; the presence of the *tert*-butoxide renders the monomer carbonyl more susceptible to nucleophilic attack. For **5** (as for inactive **2**), the presence of acetonitrile may well be detrimental, though the additional presence of phenoxide ligation in **5** appears to be a more dominant factor. Presumably the orientations adopted by the Ph_2C groups in **2** (see Fig. 4) are less favourable than in the other complexes herein which hinders monomer access in the first step of the ROP, which is reflected in the lack of activity. By contrast, the relatively poor activity observed for **1** is surprising in view of the open environments about the lithium centers, and is thought to be due to the inability of **1** to generate a lithium alkoxide. It should be noted however that this discussion of activity *versus* coordination environment/ligation is somewhat tentative given the differing nature of the Li/O ring systems present. The data here (and that for the ROP of *rac*-LA) also suggest that these catalysts require an induction period, suggestive of slow activation.

Table 1. Ring opening polymerization screening of ε-caprolactone using lithium complexes **1** – **5**.

Run	Cat	T (°C)	CL:Cat:BnOH	Time (h)	Conv[a] (%)	M_n[b] ,GPC	$M_{n,Cal}$[c]	PDI[d]
1	**1**	110	150:1:0	3	---	---	---	---
2	**1**	110	150:1:1	3	86	4170	14830	1.12
3	**2**	110	150:1:1	3	---	---	---	---
4	**2**	110	150:1:2	24	---	---	---	---
5	**3**	110	150:1:1	3	79	5790	13630	1.46
6	**3**	110	150:1:0	3	88	4440	15070	1.56
7	**3**	110	150:1:0	1	69	4310	11810	1.43
8	**4**	60	150:1:0	6	---	---	---	---
9	**4**	80	150:1:0	3	45	1860	7700	1.24
10	**4**	110	150:1:0	1	52	3360	8900	1.22
11	**4**	110	150:1:1	3	74	5470	12780	1.21
12	**4**	110	100:1:0	3	59	2890	6730	1.13
13	**4**	110	150:1:0	3	70	4560	11980	1.17
14	**4**	110	200:1:0	3	70	10350	15980	1.19
15	**4**	110	250:1:0	3	71	13390	20260	1.23
16	**4**	110	300:1:0	3	82	15580	28080	1.66
17	**4**	110	350:1:0	3	88	32690	35160	1.58
18	**4**	110	150:1:0	24	91	7430	15580	1.48
19	**5**	110	150:1:0	1	76	2530	13010	1.12
20	**5**	110	150:1:0	3	82	9360	14040	1.31

[a] Determined by ^{1}H NMR spectroscopy; [b] M_n GPC values corrected considering Mark-Houwink factors (0.56 poly(ε-caprolactone)) from polystyrene standards in THF. [c] Calculated from ($[Monomer]_0/[Cat]_0$) x conv.(%) x Monomer molecular weight. [d] From GPC.

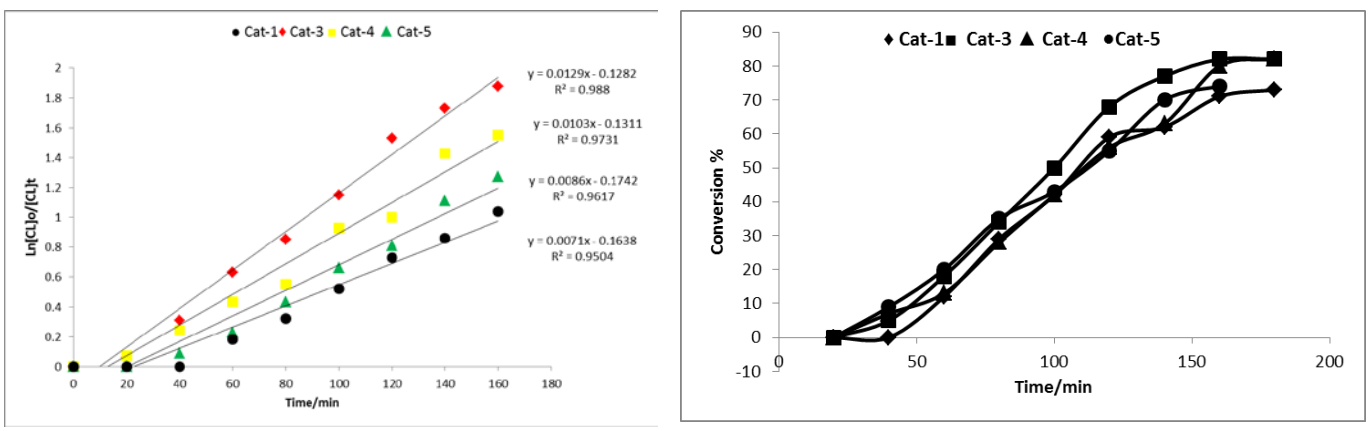

Figure 10. Left: Kinetic plots for ε-CL ROP using Li catalysts **1** and **3 - 5**; Right: Relationship between conversion and time for ε-CL ROP using **1** and **3 - 5**.

ROP of *rac*-lactide

Complexes **1** to **5** have also been screened for the ROP of *rac*-lactide, with, in the case of **1**, addition of benzyl alcohol (BnOH). Here, complex **3** was selected to determine the optimized conditions (table 2). It was observed that at temperatures below 110 ^{o}C, these systems were generally inactive even after 24 h. However, at 110 ^{o}C, a linear relationship between average molecular weight and monomer mole ratio was observed for **3** (figure S 13), whilst there is a near exponential relationship between monomer conversions and M_n values, possibly due to severe catalyst decomposition; molecular weight distributions [1.14 – 1.43] that suggest there is some degree of control. The ^{1}H NMR spectra of the PLA (table 2, runs 14; figures S15 and S16, SI) are consistent with the presence of O*t*Bu/OH end groups when the ROP is conducted in the absence of BnOH and BnO/OH end groups when conducted in the presence of BnOH). The MALDI-TOF spectrum for PLA using **1** (figure S17, SI; run 1, table 2) comprises a series of peaks separated by 72 Da with end groups OBn and ONa, for example with n = 82 = 6040 Da.

For runs conducted in the absence of BnOH, the MALDI-TOF spectrum for the PLA (figure S18, SI; run 14, table 2) is more bimodal in structure, and comprises a sizeable fraction of oligomers with peak separation 72 Da and end groups of ONa and OH; for the higher molecular weight fraction, the peak separation is 144 Da. To determine the stereo-chemical microstructure of the resulting PLA, homonuclear decoupled ^{1}H NMR spectra were recorded of the methine region, and the results revealed that the polymers were atactic (figures S19 - S21, SI). [11a] Results using 2D *J*-resolved ^{1}H NMR spectroscopy (figure S22, SI), and assignment of peaks by reference to the literature.[11b]

From a kinetic study of the ROP of *rac*-LA using **1, 3 - 5** (figure 11) at 110 ^{o}C, it was observed that the polymerization rate exhibited a first order dependence on the *rac*-LA concentration (figure 11, left), and the monomer conversion reached >70 % over 8 h (figure 11, right). The same activity trend as observed for the ROP of ε-CL was observed here (table S3).

Table 2. ROP screening of *rac*-lactide using **1** – **5**.

Run	Cat	T (°C)	*rac*-LA:Cat:BnOH	Time (h)	Conv[a] (%)	M_n[b] ,GPC	$M_{n,Cal}$[c]	PDI[d]
1	**1**	110	100:1:1	12	63	4360	9190	1.09
2	**2**	110	100:1:1	12	---	---	---	---
3	**3**	60	100:1:1	24	---	---	---	---
4	**3**	80	100:1:0	12	23	1370	3310	1.15
5	**3**	110	100:1:0	3	---	---	---	---
6	**3**	110	100:1:0	6	33	1460	4760	1.34
7	**3**	110	50:1:0	12	19	690	1370	1.17
8	**3**	110	100:1:0	12	61	3970	8790	1.14
9	**3**	110	150:1:0	12	63	4620	13620	1.19
10	**3**	110	200:1:0	12	65	6160	18740	1.18
11	**3**	110	250:1:0	12	71	7820	25580	1.17
12	**3**	110	100:1:0	24	73	5780	10520	1.24
13	**3**	150	100:1:0	12	62	3470	8936	1.43
14	**4**	110	100:1:0	12	69	6990	9940	1.15
15	**5**	110	100:1:0	12	65	4700	9370	1.18

[a] Determined by ^{1}H NMR spectroscopy; [b and d] From GPC, M_n GPC values corrected considering Mark-Houwink factors (0.58 poly (*rac*-lactide)) from polystyrene standards in THF. [c] Calculated from ([Monomer]$_0$/[Cat]$_0$) × conv.(%) × Monomer molecular weight.

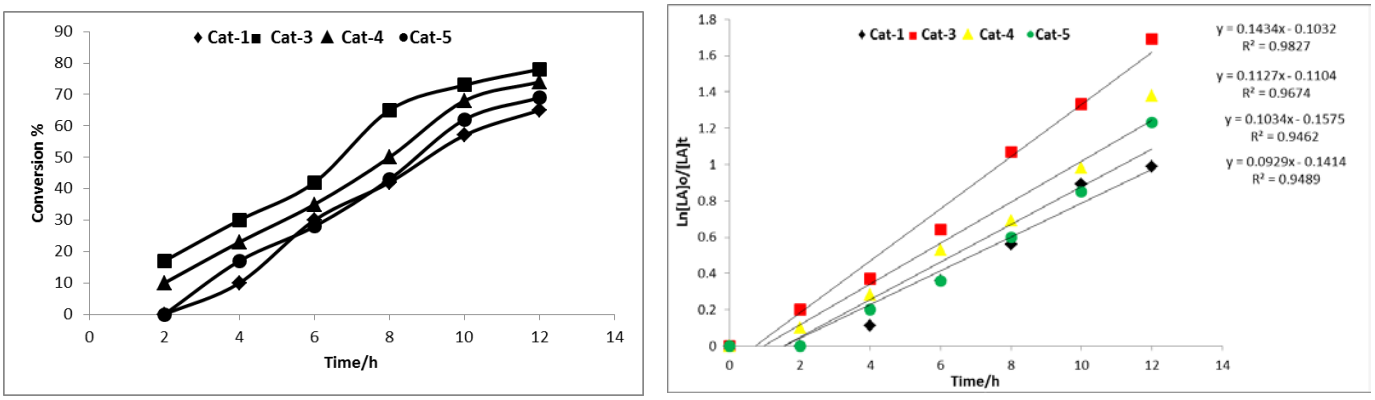

Figure 11. Left: Plot of ln[*rac*-LA]$_o$/[*rac*-LA]$_t$ *vs* time using **1** and **3 - 5**; Right: Relationship between conversion and time of polymerization *rac*-LA using **1** and **3 - 5**.

Ring Opening Polymerization (ROP) of δ-valerolactone

Complexes **1** – **5** were also evaluated as catalysts for the ROP of δ-valerolactone (table 3). The relationship between M_n and PDI and monomer mole ratio (figure S23, SI) are near linear using catalyst system **3**. ^{1}H NMR spectra of the resultant PVL (*e.g.* figure S24, SI) formed in the presence of BnOH revealed the

presence of benzyloxy and hydroxy end groups. In the absence of BnOH (*e.g.* figure S25, SI), only the end groups OH/ONa are present; the presence of a peak at c.a. 4.3 ppm suggests the absence of cyclic PLA. [12] The MALDI-TOF spectrum of the PVL (run 7, table 3, figure S26, SI) revealed a family of peaks separated by 100 Da (the molecular weight of the monomer), consistent with the presence of only oligomeric PVL. A kinetic study using **1** and **3 - 5** (figure 12) at 110 ^{o}C revealed that the polymerization rate of the ROP of δ-valerolactone exhibited a first order dependence on the δ-valerolactone concentration (figure 12, left). The monomer conversion was >70 % over 8 h (figure 12, right) and the activity trend was as observed for the ROP of ε-CL and *rac*-LA (table S3).

Table 3. ROP of δ-valerolactone using lithium complex **1 - 5**

Run[a]	Cat	δ–VL:Cat:BnOH	Time/h	Conv.%[b]	M_n[c]	$M_{n,Cal}$[d]	PDI[e]
1	**1**	100:1:1	12	61	2760	6210	1.20
2	**2**	100:1:1	12	---	---	---	---
3	**3**	50:1:0	12	43	1170	2150	1.89
4	**3**	100:1:0	12	62	1580	6200	1.91
5	**3**	150:1:0	12	64	2240	9600	1.87
6	**3**	200:1:0	12	63	4870	12600	2.15
7	**3**	250:1:0	12	64	5690	16000	1.74
8	**3**	100:1:0	24	72	6790	7200	1.99
8	**4**	100:1:0	12	66	4530	6600	1.17
9	**5**	100:1:0	12	59	3780	5900	1.19

[a] Runs conducted in toluene at 110 °C. [b] Determined by ^{1}H NMR spectroscopy; [c, e] From GPC. [d] Calculated from ([Monomer] /[Cat]) × conv.(%) × monomer molecular weight + molecular weight of BnOH.

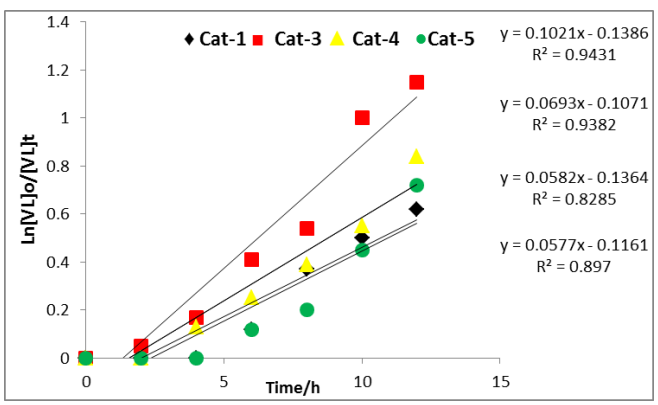

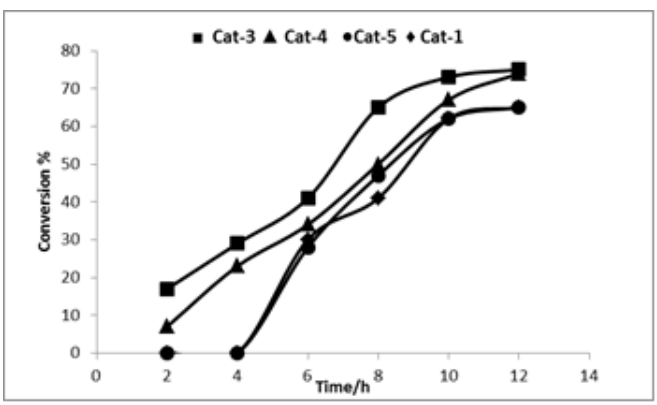

Figure 12. Left: Plot of $\ln[\delta\text{-VL}]_o/[\delta\text{-VL}]_t$ *vs* time using **1** and **3 - 5**; Right: Relationship between conversion and time of ROP of δ-VL using **1** and **3 - 5**.

Finally, the attempted co-polymerization of ε-CL and *rac*-LA was attempted (and the reverse addition), but this resulted in only homo-polymerization and isolation of PCL.

In conclusion, the use of the acids 2,2′-$Ph_2C(X)(CO_2H)$, where X = OH, NH_2, in combination with lithium *tert*-butoxide or phenoxide results in the formation of multi-metallic assemblies incorporating a variety of structural motifs such as chains, open cubes, capsules and ladders based on Li-O repeat units. For the ring opening polymerization (ROP) of ε-caprolactone (ε-CL), *rac*-lactide (*rac*-LA) and δ-valerolactone (δ-VL), all complexes except **2** were active, requiring in the case of **1**, the presence of BnOH. The polymerizations afforded products with molecular weights much lower than the calculated values, but with relatively narrow molecular weight distributions (< 2.0). Kinetic studies indicated the rate order **3** > **4** > **5** > **1**, and a first order dependence on the monomer concentration as well as an induction period (slow activation). Tentative structure active relationships are proposed such as the presence of O-*t*Bu and/or THF ligation being beneficial *versus* acetonitrile ligation being detrimental.

Supported Information Summary: Experimental section including syntheses of **1** – **5**; polymerization procedures; alternatives views of the molecular structures of **1** – **5**; graphs and NMR spectra for the ROP studies.

Acknowledgements–The National Mass Spectrometry Service at Swansea and Dr Kevin Welham (University of Hull) are both thanked for mass spectrometry data. We thank the EPSRC X-ray Crystallographic Service at the University of Southampton for data for **1′**, **2**, **3**, **4** and **5**. We wish to

acknowledge the use of the EPSRC's Chemical Database Service hosted by the RSC. The higher committee for education development in Iraq is thanked for financial support.

Keywords: Benzilic acid; Diphenylglycine; Lithium; Ring Opening Polymerization; Structures.

References

[1] See for example a) E. Chiellini, R. Solaro, *Adv. Mater*. **1996**, *8*, 305-313. b) M. A. Woodruff, D. W. Hutmacher, *Prog. Polym. Sci*. **2010**, *35*, 1217-1256. c) H. Tian, Z. Tang, X. Zhuang, X. Chen, X. Jing, *Prog. Polym. Sci*. **2012**, *37*, 237-280.

[2] a) C. K. Williams, *Chem. Soc. Rev*. **2007**, *36*, 1573-1580. b) A. Arbaoui, C. Redshaw, *Polym. Chem*. **2010**, *1*, 801-826. c) W. Alkarekshi, A. P. Armitage, O. Boyron, C. J. Davies, M. Govere, A. Gregory, K. Singh, G. A. Solan, *Organometallics*, **2013**, *32*, 249-259 and references therein. d) Y. Liu, W. -S. Dong, J. -Y. Liu, Y. -S. Li, *Dalton Trans.* **2014**, *43*, 2244-2251.

[3] a) C. Redshaw, M. R. J. Elsegood, K. E. Holmes, *Angew Chemie, Int. Ed.* **2005**, *44*, 1850-1853.

b) C. Redshaw, M. R. J. Elsegood, *Angew Chemie, Int. Ed*. **2007**, *46*, 7453-7457.

[4] M. Braun, *Angew Chemie*. **1996**, *108*, 565-568; *Angew Chemie. Int. Ed*. **1996**, *35*, 519-522.

[5] X. Wang, K. –Q. Zhao, S. Mo, Y. Al-Khafaji, T. J. Prior, M. R. J. Elsegood, C. Redshaw, unpublished results.

[6] A search of the CSD for the $Ph_2C(X)$ motif (X = O, NH) afforded 31 hits, the majority of which (80 %) were organic compounds; CSD system: F. H. Allen, *Acta Cryst.*, **2002**, *B58*, 380-388.

[7] A. K. Sutar, T. Maharana, S. Dutta, C. –T. Chen, C. –C. Lin, *Chem. Soc. Rev*. **2010**, *39*, 1724-1746.

[8] a) B. –T. Ko, C. –C. Lin, *J. Am. Chem. Soc*. **2001**, *123*, 7973-7977. b) M. H. Chisholm, C. –C. Lin, J. C. Gallucci, B. –T. Ko, *Dalton Trans*. **2003**, 406-412. c) C. –A. Huang, C. –T. Chen, *Dalton Trans*. **2007**, 5561-5566. d) W. Clegg, M. G. Davidson, D. V. Graham, G. Griffen, M. D. Jones, A. R. Kennedy, C. T.

O'Hara, L. Russo, C.M. Thomson, *Dalton Trans*. **2008**, 1295-1301. e) Y. Huang, Y. –H. Tsai, W. –C. Hung, C. –S. Lin, W. Wang, J. –H. Huang, S. Dutta, C. –C. Lin, *Inorg. Chem*. **2010**, *49*, 9416-9425. f) W. –Y. Lu, M. –W. Hsiao, S. C. N. Hsu, W. –T. Peng, Y. –J. Chang, Y. –C. Tsou, T. –Y. Wu, Y. –C. Lai, Y. Chen, H. –Y. Chen, *Dalton Trans*. **2012**, *41*, 3659-3667. g) N. Ikpo, C. Hoffmann, L. N. Dawe, F. M. Kerton, *Dalton Trans*. **2012**, *41*, 6651-6660. h) R. K. Dean, A. M. Reckling, H. Chen, L. N. Dawe, C. M. Schneider, C. M. Kozak, *Dalton Trans*. **2013**, *42*, 3504-3520. i) Z. Liu, H. –X. Chen, D. Huang, Y. Zhang, Y. –M. Yao, *J. Organomet. Chem*. **2014**, *749*, 7-12. j) L. N. Saunders, L. N. Dawe, C. M. Kozak, *J. Organomet. Chem*. **2014**, *749*, 34-40. k) D. Alhashmialameer, N. Ikpo, J. Collins, L. N. Dawe, K. Hattenhauer, F. M. Kerton, *Dalton Trans*. **2015**, *44*, 20216-20231. l) S. Ghosh, D. Chakraborty, B. Varghese, *Eur. Polym. J*. **2015**, *62*, 51-65. m) J. Char, O. G. Kulyk, E. Brulé, F. de Montigny, V. Guérineau, T. Roisnel, M. J. –L. Tschan, C. M. Thomas, *C. R. Chimie*, **2016**, *19*, 167-172.

[9] As of 01.09.16, the price of benzilic acid is £13.50 for 100 g, whereas 2,2′-diphenylglycine costs £92.80 for 5 g (prices do not include VAT). Source SigmaAldrich.com.

[10] H. Nakajima, M. Yasuda, A. Baba, *Dalton Trans*. **2012**, *41*, 6602-6606 and references therein.

[11] a) P. Piromjitpong, P. Ratanapanee, W. Thumrongpatanaraks, P. Kongsaeree, K. Phomphrai, *Dalton Trans*. **2012**, *41*, 12704-12710. b) M. J. Walton, S. J. Lancaster, C. Redshaw, *ChemCatChem*. **2014**, *6*, 1892-1898 and references therein.

[12] E. Piedra-Arroni, C. Ladaviére, A. Amgoune, D. Bourissou, *J. Am. Chem. Soc*. **2013**, *135*, 13306-13309.

Table 4. Crystallographic data for complexes **1**·2C_4H_8O, **1′** and **2**·2MeCN·THF.

Compound	**1**·2C_4H_8O	**1′**	**2**·2MeCN·THF
Formula	$C_{28}H_{22}Li_2O_6$·2C_4H_8O	$C_{18}H_{19}LiO_4$	$C_{108}H_{94}Li_7N_3O_{22}$
Formula weight	611.8	306.27	1834.44
Crystal system	Orthorhombic,	Orthorhombic	Monoclinic
Space group	*Pna*2$_1$	*P*2$_1$2$_1$2$_1$	*P*2$_1$/*n*
Unit cell dimensions			
a (Å)	10.099(2)	5.8603(12)	14.9367(10)
b (Å)	12.685(3)	16.286(4)	27.942(2)
c (Å)	24.611(6)	17.064(4)	23.4063(16)
α (º)	90	90	90
β (º)	90	90	105.2360(10)
γ (º)	90	90	90
V (Å^3)	3152.8(19)	1628.6(6)	9425.5(11)
Z	4	4	4
Temperature (K)	100 K	100(2)	100(2)
Wavelength (Å)	0.71073	0.71075	0.6889
Calculated density (g.cm^{-3})	1.283	1.249	1.293
Absorption coefficient (mm^{-1})	0.09	0.09	0.09
Transmission factors (min./max.)	0.982and 0.997	0.984 and 0.996	0.776 and 1.000
Crystal size (mm^3)	0.70 × 0.07 × 0.03	0.19× 0.17 × 0.04	0.20 × 0.04 × 0.03
θ(max) (°)	30.2	30.1	27.6
Reflections measured	21169	12859	90603
Unique reflections	7745	4342	21513
R_{int}	0.036	0.021	0.077
Reflections with $F^2 > 2\sigma(F^2)$	7140	4342	90603
Number of parameters	421	215	1248
R_1 [$F^2 > 2\sigma(F^2)$]	0.053	0.044	0.053
wR_2 (all data)	0.105	0.099	0.130
GOOF, *S*	1.07	1.04	1.03
Largest difference peak and hole (e Å^{-3})	0.24 and –0.25	0.33 and –0.33	0.42 and –0.41

Table 4 con't. Crystallographic data for complexes **3**, **4** and **5**.

Compound	3	4	5
Formula	$C_{116}H_{128}Li_8O_{22}$	$C_{72}H_{82}Li_6N_4O_{12}$	$C_{88}H_{80}Li_8N_8O_{12}$
Formula weight	1929.70	1237.06	1497.12
Crystal system	Triclinic	Triclinic	Tetragonal
Space group	$P\ \bar{1}$	$P\ \bar{1}$	$P\ \bar{4}$
Unit cell dimensions			
a (Å)	13.402(5)	11.5582(17)	16.1256(7)
b (Å)	13.466(4)	12.9469(19)	16.1256(7)
c (Å)	17.306(8)	13.1142(19)	15.3363(9)
α (º)	68.55(3)	118.444(8)	90
β (º)	75.65(4)	101.424(7)	90
γ (º)	64.93(4)	92.831(7)	90
V (Å^3)	2617(2)	1667.7(4)	3988.0(4)
Z	1	1	2
Temperature (K)	100(2)	100(2)	100(2)
Wavelength (Å)	0.71073	0.71073	0.71073
Calculated density (g.cm^{-3})	1.224	1.232	1.247
Absorption Coefficient t(mm^{-1})	0.08	0.08	0.08
Transmission factors (min./max.)	0.740 and 1.000	0.986 and 0.998	0.63629 and 1.000
Crystal size (mm^3)	0.13× 0.09 × 0.03	0.18 × 0.05× 0.20	0.04 × 0.03 × 0.02
θ(max) (°)	25.0	25.00	26.145
Reflections measured	22115	13706	16772
Unique reflections	9154	5859	7856
R_{int}	0.078	0.134	0.068
Reflections with $F^2 > 2\sigma(F^2)$	6016	3464	16772
Number of parameters	664	439	494
R_1 [$F^2 > 2\sigma(F^2)$]	0.046	0.098	0.091
wR_2 (all data)	0.268	0.245	0.239
GOOF, S	1.146	0.991	1.022
Largest difference peak and hole (e Å^{-3})	0.32 and –0.36	0.29 and –0.30	0.49 and –0.40